Available online at www.sciencedirect.com
ScienceDirect
Thin Solid Films 515 (2007) 3073–3078
thin solid films
www.elsevier.com/locate/tsf

Post-annealing temperature dependence of infrared absorption enhancement of polymer on evaporated silver films

Y. Suzuki [a,*], Y. Ojima [a], Y. Fukui [a], H. Fazyia [a], K. Sagisaka [b]

[a] Department of Advanced Physics, Faculty of Science and Technology, Hirosaki University, Hirosaki 036-8561, Japan
[b] Nanomaterials Laboratory, National Institute for Materials Science, 1-2-1 Sengen, Tsukuba, Ibaraki 305-0047, Japan

Received 20 December 2005; received in revised form 31 July 2006; accepted 29 August 2006
Available online 9 October 2006

Abstract

Infrared absorption spectra were measured at normal incidence of radiation for polymers on post-annealed silver films of 4–10 nm mass thicknesses that had been deposited in ultra high vacuum onto Si substrate surfaces. Results show that the polymer absorption intensity depends on the annealing temperature and the silver mass thickness.

Results clarified that no simple relation existed, such as a negative correlation between reflectivity and the infrared absorption enhancement, even when the mass thickness was made constant and the silver particles' size and shape were changed. For infrared absorption intensity to become large, particles must be positioned discretely, but if the distance between particles is too large, absorption intensity decreases. Moreover, results verified that optimal thin-film morphology was different according to the wavelength region.

Keywords: Infrared spectroscopy; Optical properties of thin films; Silver inland film; Infrared absorption enhancement

1. Introduction

Silver films that are evaporated onto dielectric substrates enhance infrared absorption of surface molecules [1–12]. Most investigations have concluded that physical effect of the absorption enhancement can be caused by surface electromagnetic field enhancements associated with collective electron resonance in metal islands. However, interpretation of those enhancements remains indeterminate. Understanding the morphology of island films involved in enhancement is expected to be useful to elucidate absorption enhancement mechanisms [13,14].

Thin film deposition by the vacuum thermal evaporation presents various advantages. However, for evaporated films, the mass thickness, the film structure of the metal particle (size and shape) change simultaneously [4,5]. For that reason, it remains unclear how much each element is related to infrared absorption enhancement.

In this study, post-annealing changed only the film structure of a thin film with constant mass thickness. This study clarifies the effects of mass thickness and film structure on infrared absorption enhancement.

2. Experimental details

Silver films of 1–10 nm in mass thickness were deposited on silicon wafers using electron-beam evaporation in a vacuum chamber of 1×10^{-6} Pa at room temperature. The mass thickness of the Ag films was determined using quartz crystal oscillator (XTM/2; Leybold Inficon) placed adjacent to the Si surface. After evaporation, silver films were annealed in situ at various temperatures (50–300 °C) in an ultra high vacuum chamber (base pressure: 5×10^{-8} Pa). Each sample is kept for 1 h at the selected temperature, then cooled afterwards.

We used a styrene–maleic acid comb copolymer as absorbing material. Dropping an ethyl alcohol solution (289 mg/l) onto Ag films (40 μl on 1.44 cm^2) that had been pre-deposited on the Si wafer formed the polymer. Bulk density of 1 was assumed for polymer. Infrared absorption spectra were obtained at normal incidence of radiation using a Fourier transform infrared spectrophotometer (MB-100; ABB Bomem) averaging of 128 scans at 4 cm^{-1} resolution.

* Corresponding author. Tel./fax: +81 172 39 3556.
E-mail address: uc@cc.hirosaki-u.ac.jp (Y. Suzuki).

0040-6090/$ - see front matter © 2006 Elsevier B.V. All rights reserved.
doi:10.1016/j.tsf.2006.08.029

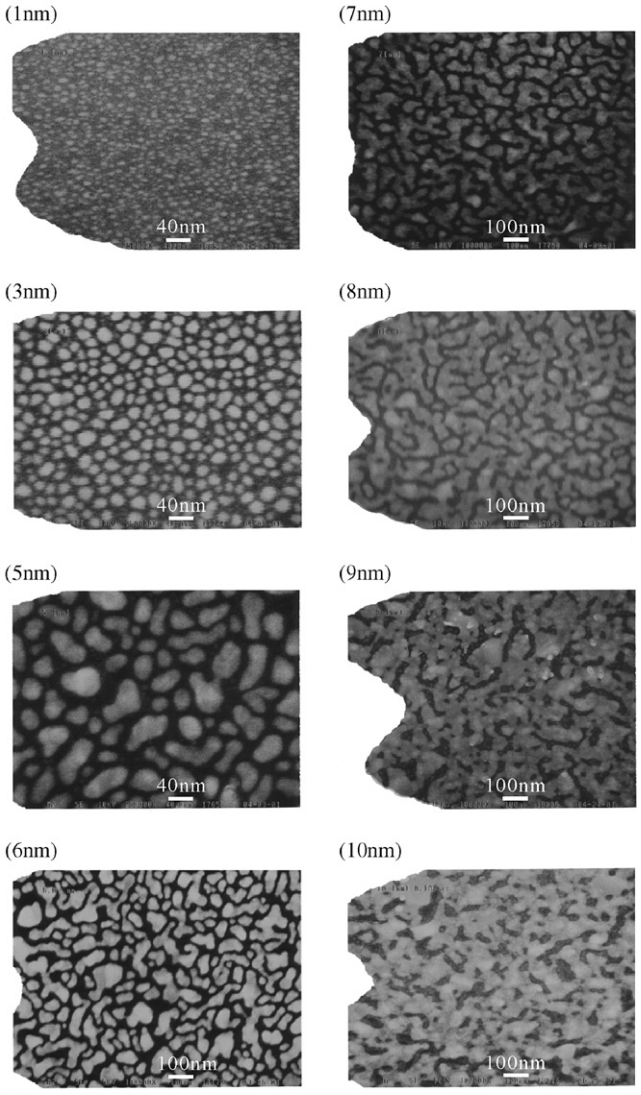

Fig. 1. Field-emission SEM micrographs of Ag films deposited on a Si wafer. Film thickness 1 nm, 3 nm, 5 nm, 6 nm, 7 nm, 8 nm, 9 nm, 10 nm.

Morphologies of the Ag films deposited on chemically oxidized Si wafer were observed with a field-emission scanning electron microscope (FE-SEM, LS-780; Topcon Corp.) and the Ag films deposited on naturally oxidized Si wafer were observed with FE-SEM (JSM-7000F; JEOL) taken at 10 keV.

3. Results and discussion

Evaporated metal films often become island-shaped films. Especially, thin noble metal films on semiconductor substrates exhibit Volmer–Weber type growth, thereby becoming island films. If the substrate temperature is raised after evaporation to such a film, mobility will be imparted to metal islands (particles) and film morphology will change greatly. Particles that achieve mobility move onto the substrate's surface, merge with other particles, and consequently become larger particles. The degree of morphological change depends on the annealing temperature. In the case of Ag thin film of 4 nm evaporated on germanium substrate at room temperature, it is an almost continuous film immediately after deposition, but it changes to discrete big particles through annealing at 200 °C for 2 h [4]. Films with various forms with identical mass thickness were produced using this phenomenon. Polymer thin films were formed on respective films, and their respective infrared absorption spectra were observed.

To elucidate the relation between the film morphology and the infrared transmittance, SEM micrograph and the infrared transmission spectra are shown in Figs. 1 and 2. Fig. 1 shows a series of FE-SEM micrographs of a silver island-shaped film deposited on chemically oxidizes Si wafer taken at 10 keV. The Ag film morphology depended largely upon thickness. The minimum thickness in our samples was 1 nm [Fig. 1 (1 nm)], at which fine Ag particles dispersed randomly on the substrate. Between thickness of 3 nm [Fig. 1 (3 nm)] and 5 nm [Fig. 1 (5 nm)], these particles were clumped into three-dimensional islands with various heights and sizes. Between thickness of 6 nm [Fig. 1 (6 nm)] and 7 nm [Fig. 1 (7 nm)], these particles were started to contact neighbors and merged into complex particles islands which are not globular any longer. When the thickness was 8 nm [Fig. 1 (8 nm)] or greater [Fig. 1 (9 nm), (10 nm)], these islands coalesced into a continuous film, but intricate-shape openings (gaps) remained in the film even at 9 nm [Fig. 1 (9 nm)] and 10 nm [Fig. 1 (10 nm)].

Fig. 2 depicts the silver film thickness dependence of infrared transmittance. The silver film thickness is 1 to 10 nm. Each transmittance value was normalized with respect to the transmittance of the Si wafer. The band at 2350 cm^{-1} is assigned to atmospheric CO_2 molecules; the bands at 4000–3500 cm^{-1}, 3200 cm^{-1}, and 1800–1300 cm^{-1} are assigned to atmospheric water vapor molecules in the optical path. When island is completely separated (1 to 5 nm), transmittance hardly decreases. For the films which are thicker than 6 nm, overall transmittance decreases with the increase in film thickness. Although transmittance decreases with the increase in wavenumber in 6 and 7 nm films, transmittance decreases by the low

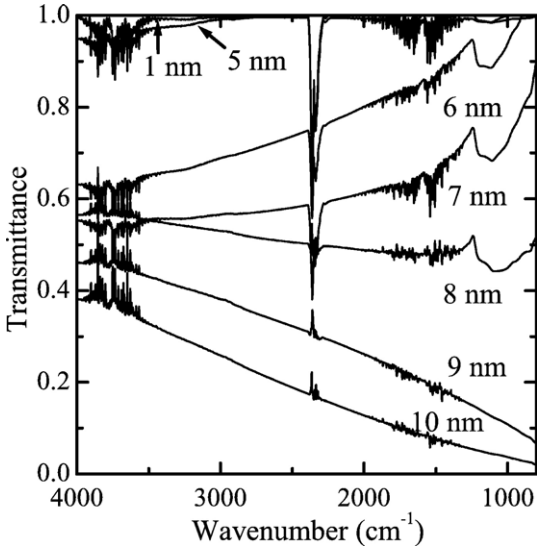

Fig. 2. Change of infrared transmission spectra with thickness of as-deposited Ag films taken at an normal incidence with respect to the bare Si wafer.

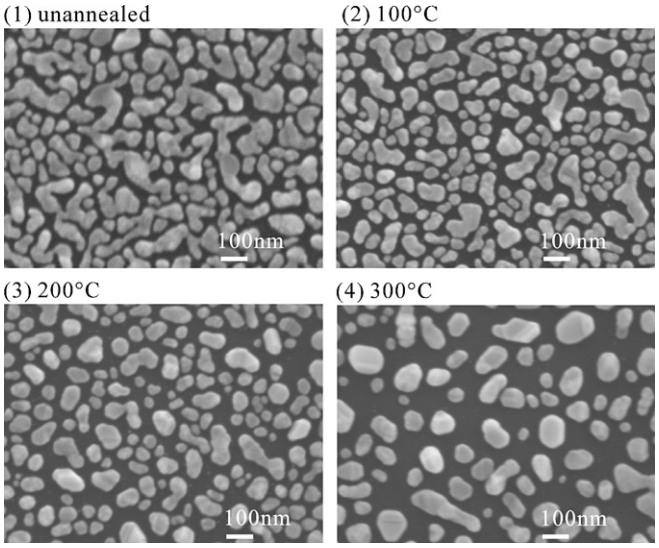

Fig. 3. Field-emission SEM micrographs of 6-nm-thick Ag films deposited on a naturally oxidized Si wafer: (1) unannealed and annealed at (2) 100 °C, (3) 200 °C, (4) 300 °C.

wavenumber side conversely for 8 to 10 nm films. The wavenumber dependence of transmittance changes with film thickness based on the influence of surface scattering and anomalous absorption by the metal film: it is considered to originate in film percolation [15,16]. Transmittance decreases concomitant with the decrease in wavenumber if the metal's dielectric constant is considered. However, transmittance on the high wavenumber side is lower in a thin film thickness because the influence of surface scattering is great. The influence of surface dispersion is large if a film is a discontinuous island film. The influence of surface scattering will become small if a film grows as a continuous film. Thereby, the film has grown to be a continuous film from an island film at about 7.5 nm, which influences its surface scattering reflectivity and reverses anomalous absorption.

To elucidate the film morphology, SEM micrographs are shown in Fig. 3. This figure shows annealing temperature dependence of FE-SEM micrographs of a 6-nm-thick silver island-shaped film deposited on naturally oxidized Si wafer taken at 10 keV. The Ag film morphology depended largely upon annealing temperature. The unannealed film has not globular structure. The particles were coalesced mutually. When the film was annealed at 100 °C, particles started to separate and the gaps between particles were enlarged. Moreover, when annealing temperature is high, the particles' shape has approached globular and the gap between particles has expanded further. The silver particle size and shape were changed according to the rise of the annealing temperature.

Fig. 4 shows infrared transmission absorption spectra of the silver films evaporated on naturally oxidized Si wafer. The silver film thicknesses are 4, 6 and 10 nm. Since the pretreatment method of substrate is different from the case of Fig. 2, the relations between the film thickness and transmittance are different from the case of Fig. 2. Annealing raises transmittance in all cases. Moreover, when annealing temperature is high, the degree of the transmittance increase is also larger. As shown in the case of as-deposited films, for 4 nm film transmittance rises according to the decrease in wavenumber. On the other hand, at 6 and 10 nm, in contrast to the case of 4 nm, transmittance decreases according to the decreased wavenumber. As mentioned above, the relation between wavenumber and transmittance has been clarified in precedent studies [15,16]. The above-mentioned evidence clarifies that the thin film in this research before annealing has a discrete island for 4 nm film; it is a near-continuous film for 6 and 10 nm films.

Fig. 5 shows infrared transmission absorption spectra of 80-nm-thick polymer adsorbed on silver films. Absorbance of ν(CH) and ν(CO) have been changed variously depending on the film thickness and annealing temperature. Transmittance is extremely low for the polymer coatings that were prepared on 10 nm Ag film that were not annealing at sufficiently high temperature.

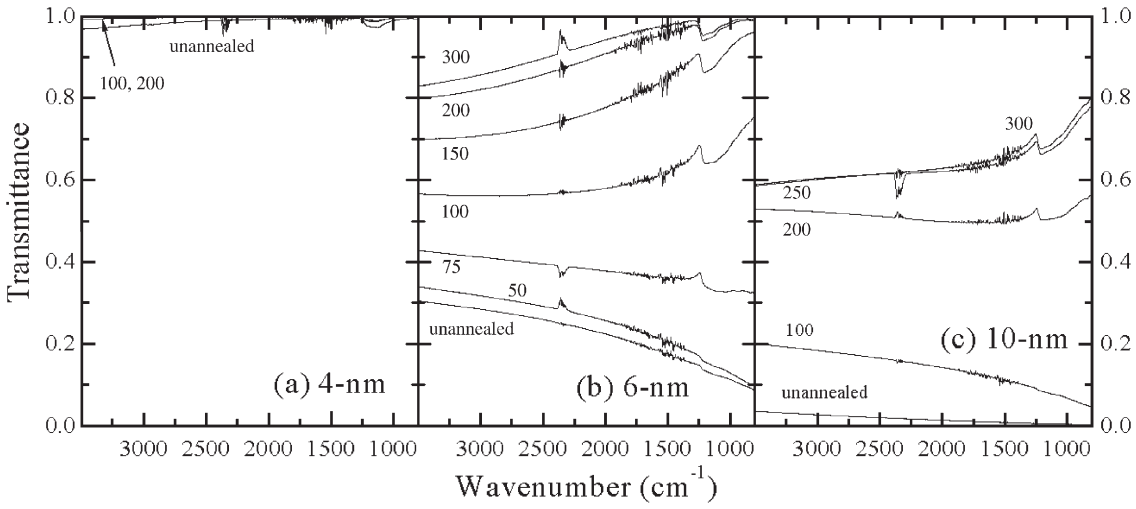

Fig. 4. Evolution of infrared transmission spectra of bare Ag films as a function of annealing temperature for (a) 4-nm-, (b) 6-nm-, and (c) 10-nm-thick films.

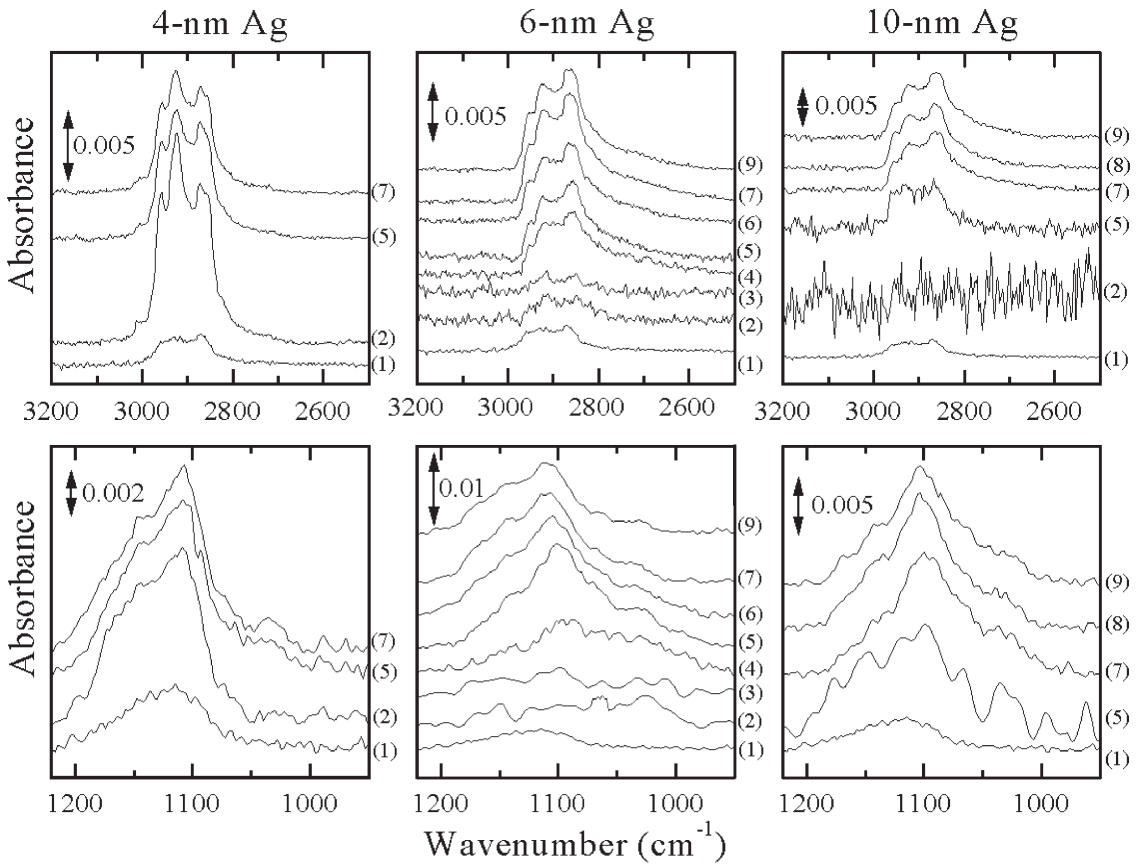

Fig. 5. Absorbance spectra of 80-nm-thick styrene–maleic acid comb polymer deposited on (a) 4-nm-, (b) 6-nm-, and (c) 10-nm-thick Ag films. Top: 3000 cm^{-1} region [ν(CH)]; bottom: 1000 cm^{-1} region [ν(CO)]. (1) No Ag, (2) unannealed, and annealed at (3) 50 °C, (4) 75 °C, (5) 100 °C, (6) 150 °C, (7) 200 °C, (8) 250 °C, and (9) 300 °C.

To ease comprehension of the film thickness and annealing temperature dependence of the absorbance, Figs. 6 and 7 present the enhancement factor the ratio of the integral absorbance value obtained between 2450 and 2990 cm^{-1} and between 1000 and 1210 cm^{-1} with an Ag underlayer and without, and the background transmittance at 2900 and 1100 cm^{-1} for

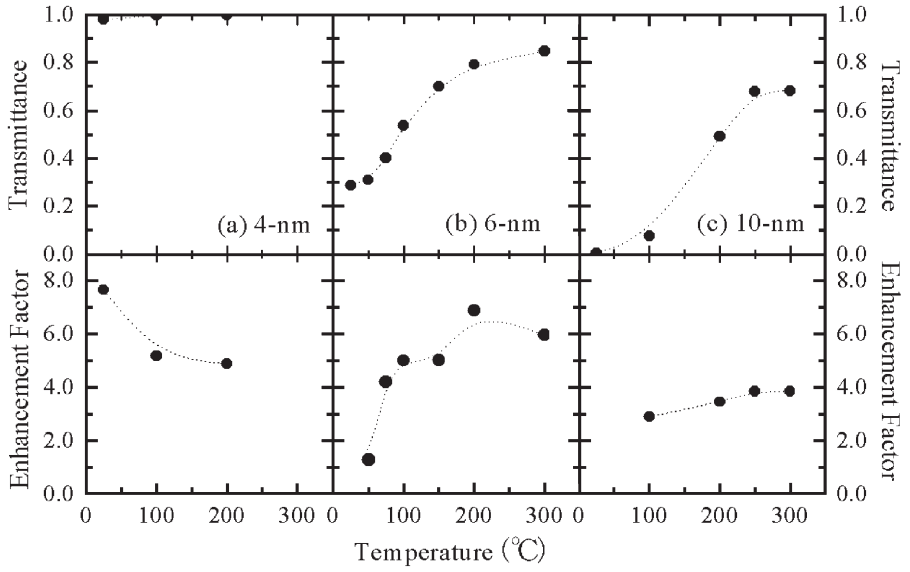

Fig. 6. Variation of absorbance of the ν(CH) of 80-nm-thick styrene–maleic acid comb polymer film and reflectivity at 2900 cm^{-1} as a function of Ag film annealing temperature for (a) 4-nm-, (b) 6-nm-, and (c) 10-nm-thick Ag films.

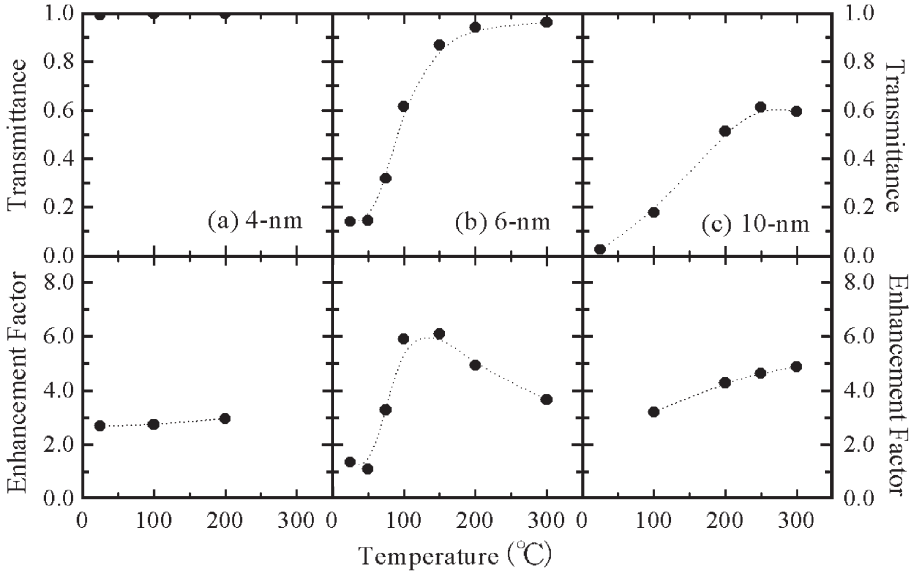

Fig. 7. Variation of absorbance of the ν(CO) of 80-nm-thick styrene–maleic acid comb polymer film and reflectivity at 1100 cm^{-1} as a function of Ag film annealing temperature for (a) 4-nm-, (b) 6-nm-, and (c) 10-nm-thick Ag films.

these Ag film thicknesses as a function of the annealing temperature. Fig. 6 shows results for the 3000 cm^{-1} region [ν(CH)]; Fig. 7 shows that for the 1000 cm^{-1} region [ν(CO)].

In the case of the 4-nm-thick Ag undelayer, the change in the transmittance with the Ag film annealing temperature was slight because the film already comprised discrete islands before annealing. Especially, transmittance is almost 100% in the 1000 cm^{-1} region, regardless of the Ag film annealing temperature. Therefore, the enhancement factor does not change significantly either with Ag film annealing temperature (Fig. 7). On the other hand, in the 3000 cm^{-1} region, the transmittance results increased very slightly as a result of annealing and enhancement factor decreased along with it. Taken together, these observations suggest that the short wavelength region is sensitive to change in the film morphology.

In the case of 6 nm, the transmittance changes dramatically with annealing. In the 3000 cm^{-1} region, the transmittance of about 30% increases to 80% or more; transmittance that is about 10% rises to about 100% in the 1000 cm^{-1} region. Moreover, as shown in Fig. 4, the positive slope of the transmission curve has changed to a negative slope by annealing. This change indicates that a continuous film became a discrete structure by annealing. It is understood from the wavenumber dependence of the transmittance that the percolation threshold is between 75 °C and 100 °C. On the other hand, the enhancement factor rises in accompaniment to the increasing annealing temperature; it decreases again afterwards. Regarding the relation between the enhancement factor and the transmittance, a negative correlation that had been reported before [13] was not apparent. The enhancement factor also increases concomitant with the rise of transmittance when the annealing temperature is comparatively low. It is similar for 4 nm: an enhancement factor of one or more is obtained when transmittance is about 100%. These facts support the results obtained in studies that have used small Au particles dispersed in polymer [17], and contradict the theory that holds: 'Energy of light absorbed to the metal generates the enhanced field'. Maximum values of the enhancement factor were from 200 °C (3000 cm^{-1} region) to 150 °C (1000 cm^{-1} region), whereas the percolation threshold obtained from the transmittance was 75–100 °C. The infrared absorption enhancement is large on the high temperature side of percolation threshold. In other words, the infrared absorption enhancement is large when a metallic film exists discretely. Moreover, annealing at a higher temperature spurs growth to form larger islands, enlarges the distance separating islands, decreases the volume fraction, and decreases infrared absorption enhancement. The decreased particle size and increasing volume fraction of metal engender the increased enhancement factor, which was shown by previous research results [17].

In the case of 10 nm, the transmittance is several percentage points; light only transmits slightly for as-deposited metal film. The transmittance reaches 50% or more by annealing to 200 °C or more. However, transmittance remained at about 70% although the annealing temperature was raised to 300 °C. The probable cause of the lack of inter-island distance growth is that the amount of the metal is large. The Fig. 1 (5 nm) clarifies that both the enhancement factor and the transmittance in the case annealed at 250 °C and the case annealed at 300 °C are nearly unchanged. Apparently, the change in the film morphology is saturated at 250 °C. Both the enhancement factor and the transmittance are increased according to the increase of the annealing temperature till 250 °C. This can be explained by inferring that the change in the film morphology (island growth) was saturated at about 250 °C. It can be said that in 10 nm this temperature is a little bit higher than percolation threshold. That such a state obtains the maximum enhancement factor resembles the case of 6 nm.

Two causes can be considered for the wavenumber dependence of infrared absorption intensity [18,19] on silver film thickness. One is that the dielectric constant of silver

depends on the wavenumber. The other is that the relative value to the incidence wavelength of the film constants (the Ag film thickness, the particle size, and the distance separating particles) depends on the wavenumber. The dielectric constant is large on the lower wavenumber side. Also, the effective dielectric constant of the thin film generally becomes smaller than the bulk value. Examining the above phenomenon, the relative values to the incident wavelength are inferred as a major cause.

4. Summary

In this study, post-annealing changed the film structure (size and shape) of the thin film with a constant mass thickness. This study was intended to clarify the respective effects of mass thickness and the particle size and shape on infrared absorption enhancement.

Silver thin films of 4, 6, and 10 nm were deposited on Si substrate and were annealed in vacuum for 1 h from 50 to 300 °C. Results showed no simple relation, such as a negative correlation between reflectivity and the infrared absorption enhancement, even when the mass thickness was made constant and the silver particle size and shape were changed. Consequently, we confirmed that energy of the light absorbed to the metal did not necessarily generate the enhanced field.

The maximum infrared absorption intensity is observed regardless of the mass film thickness when the annealing temperature is higher than the percolation threshold. That is, when the effect of surface scattering was larger than anomalous absorption (i.e., when Ag particles form a thin film with the crevice), it became clear that infrared absorption intensity became maximal.

Moreover, it was confirmed that optimal thin film morphology differed according to the wavelength region, perhaps because the relative values to incident wavelength of the particle size, along with other factors, depend on the wavenumber.

References

[1] A. Hartstein, J.R. Kirtley, J.C. Tsang, Phys. Rev. Lett. 45 (1980) 201.
[2] A. Hatta, T. Ohshima, W. Suëtaka, Appl. Phys., A 29 (1982) 71.
[3] A. Hatta, Y. Suzuki, W. Suëtaka, Appl. Phys., A 35 (1984) 135.
[4] Y. Suzuki, H. Seki, T. Inamura, T. Tanabe, T. Wadayama, A. Hatta, Surf. Sci. 427–428 (1999) 136.
[5] Y. Suzuki, H. Seki, T. Inamura, T. Tanabe, T. Wadayama, A. Hatta, Surf. Sci. 433–435 (1999) 261.
[6] T. Tanabe, Y. Suzuki, A. Hatta, Phys. Low-Dimens. Struct. 10 (1997) 13.
[7] Y. Suzuki, K. Kita, N. Matsumoto, Phys. Low-Dimens. Struct. 1/2 (2001) 1.
[8] Y. Suzuki, K. Kita, N. Matsumoto, Appl. Phys., A 77 (2003) 613.
[9] Y. Suzuki, N. Matsumoto, T. Ainai, T. Miyanaga, H. Hoshin, Polyhedron 24 (2005) 685.
[10] T. Kamata, A. Kato, J. Umemura, T. Takenaka, Langmuir 3 (1987) 1150.
[11] S. Badilescu, P.V. Ashrit, V.-V. Truong, Appl. Phys. Lett. 52 (1988) 1551.
[12] Y. Nishikawa, K. Fujiwara, T. Shima, Appl. Spectrosc. 45 (1991) 747.
[13] M. Osawa, Bull. Chem. Soc. Jpn. 70 (1997) 2861.
[14] T. Wadayama, O. Suzuki, K. Takeuchi, H. Seki, T. Tanabe, Y. Suzuki, A. Hatta, Appl. Phys., A 69 (1999) 77.
[15] M. Sinther, A. Pucci, A. Otto, A. Priebe, S. Diez, G. Fahsold, Phys. Status Solidi, A Appl. Res. 188 (2001) 1471.
[16] Y. Suzuki, S. Goto, H. Umetsu, Eur. J. Phys. D 33 (2005) 201.
[17] Y. Suzuki, H. Makanae, H. Kudo, T. Miyanaga, T. Nanke, T. Kobayashi, Appl. Phys., A 78 (2003) 335.
[18] G.I. Dovbeshko, V.I. Chegel, N.Y. Gridina, O.P. Repnytska, Semicond. Phys. Quantum Electron. Optoelectron 4 (2001) 202.
[19] G.I. Dovbeshko, in: G.O. Puchkovska, T.A. Gavrilko, O.I. Lizengevich (Eds.), XVI International Conference on Spectroscopy of Molecules and Crystals, Sevastopol, Ukraine, May 25–June 1, 2003, Proceedings of SPIE 5507 (2004) 386.